Trop. J. of Eng., Sci. and Techn. 2022. 1(1):149-167
@Tropical Journal of Engineering, Science and Technology.

Synthetic Anthraquinone Vat Dye Removal on NaCl-activated Agro Biomass: Process Characterisation and Modelling

Chinenye Adaobi Igwegbe[1*], Chinedu Josiah Umembamalu[1]
[1]*Department of Chemical Engineering, Nnamdi Azikiwe University, P.M.B. 5025, Awka 420218, Niger*
[*]**Corresponding author**: ca.igwegbe@unizik.edu.ng,
chinenyeigwegbe@gmail.com,+2348036805440

Abstract

Water pollution caused by the discharge of coloured effluents from dye-using industry is one of the world's main environmental challenges today. Dyes are mutagenic and carcinogenic, producing significant effects on the neurological system, reproductive system, liver, brain, and kidney; hence, they must be removed from water before disposal. The carbon from activated African pear seeds (CAPS) is used to remove Golden Yellow (GY) from its aqueous solution. To find the best conditions, the adsorption removal of GY on CAPS was modelled using the response surface methodology (RSM) via Central Composite Design (CCD). The RSM and artificial neural network (ANN) approaches were used to simulate the process, and their predictive capabilities were compared. Contact period of 78.13 min, solution temperature of 313.57K, pH of solution: 4.24, and adsorbent dosage of 0.88 g led to 77.77% removal with the desirability of 1. The high values of R^2 (0.9879), adjusted R^2 (0.9767), and anticipated R^2 (0.9307) indicated that the RSM model can represent the elimination of GY dye with CAPS. The high R^2 value (0.9943) and statistical functional errors given by the artificial neural network modelled data depicted a more adequate correlation than the RSM. RSM may be used to optimise and characterise the removal of GY from aquatic environments since the experimental (77.93%) at the optimum settings is close to the predicted (77.77%) value. The mathematical models derived from the statistical analysis can be used to improve process conditions.

Keywords: Adsorption; Biomass conversion; *Dacroydes edulis*; Optimisation; Response surface methodology; Waste water purification

Élimination synthétique du colorant de la cuve de la cuve de la cuve de la TVA sur la biomasse agro-activée par le NaCl: caractérisation et modélisation du processus

Résumé

La pollution de l'eau causée par la décharge d'effluents colorés de l'industrie de l'utilisation des colorants est l'un des principaux défis environnementaux du monde aujourd'hui. Les colorants sont mutagènes et cancérigènes, produisant des effets significatifs sur le système neurologique, le système reproducteur, le foie, le

cerveau et les reins; Par conséquent, ils doivent être retirés de l'eau avant l'élimination. Le carbone des graines de poire africain activées (CGPA) est utilisée pour éliminer le jaune doré (JD) de sa solution aqueuse. Pour trouver les meilleures conditions, l'élimination de l'adsorption de JF sur CAPS a été modélisée en utilisant la méthodologie de surface de réponse (MSR) via la conception composite centrale (CCC). Les approches MSR et le réseau neuronal artificiel (RNA) ont été utilisées pour simuler le processus, et leurs capacités prédictives ont été comparées. Période de contact de 78,13 min, température de la solution de 313,57k, pH de solution: 4,24 et posologie adsorbante de 0,88 g a conduit à 77,77% d'élimination avec l'opportunité de 1. Les valeurs élevées de R^2 (0,9879), ajustées R2 (0,9767), et R2 prévu (0,9307) a indiqué que le modèle MSR peut représenter l'élimination du colorant JD avec CGPA. La valeur R^2 élevée (0,9943) et les erreurs fonctionnelles statistiques données par les données modélisées par le réseau neuronal artificiel représentaient une corrélation plus adéquate que le MSR. MSR peut être utilisé pour optimiser et caractériser l'élimination de JD des environnements aquatiques, car la valeur expérimentale (77,93%) aux paramètres optimaux est proche de la valeur prévue (77,77%). Les modèles mathématiques dérivés de l'analyse statistique peuvent être utilisés pour améliorer les conditions de processus.

Mots-clés: adsorption; Conversion de biomasse; *Dacroydes Edulis*; Optimisation; Méthodologie de surface de réponse; Purification des eaux usées

إزالة الصبغة الاصطناعية انتزقحنون الكتلة الزراعية المنشطة : توصيف

العملية و النمذجة

نبذة مختصرة

يعدتل وثال مياها لناجمعن تصريف النفايات السائلة الملونة من الصناعة التيتستخدم الأصباغ أحد التحديات البيئية الرئيسية في العالم اليوم. الأصباغ مطفرة ومسببة للسرطان، ولها تأثير اتكبيرة على الجهاز العصبي، والجهاز التناسلي، والكبد، والدماغ، والكلى .ومنثم، يجب إزالتها من الماء قبل التخلص منها .يستخدم الكربون من بذور الكمثرى الأفريقية المنشطة (CAPS) لإزالة اللون الأصفر الذهبي (GY) من محلولها المائي. للعثور على أفضل الظروف، تمتنمذجة إزالة امتصاص GY على CAPS باستخدام منهجية سطح الاستجابة (RSM) عبر التصميم المركب المركزي .(CCD)تم استخدام نهج RSM والشبكة العصبية الاصطناعية (ANN) لمحاكاة العملية، وتمت مقارنة قدراتهما التنبؤية. أدت فترة الاتصال البالغة 78.13 دقيقة، ودرجة حرارة المحلول 313.57 كل فن، ودرجة الحموضة للمحلول : 4.24، وجرعة الممتزات البالغة 0.88 جم إلى إزالة 77.77 ٪ باستحسان .1 تشير القيم العالية لـ (0.9879) R2 و R2المعدلة (0.9767) و R2 المتوقعة (0.9307) إلى أن نموذج RSM يمكن أن يمثل إزالة صبغة GY باستخدام .CAPSأظهرت قيمة R2 العالية (0.9943) والأخطاء الوظيفية الإحصائية التي قدمتها البيانات النموذجية للشبكة العصبية الاصطناعية ارتباطًا أكثر ملاءمة من .RSM يمكن استخدام RSM لتحسين وتوصيف إزالة GY من البيئات المائية حيث أن التجربة (77.93%) في الإعدادات المثلى قريبة من القيمة المتوقعة (77.77%)، ويمكن استخدام النماذج الرياضية المشتقة من التحليل الإحصائي لتحسين شروط العملية.

الكلمات الرئيسية: امتزاز ؛ تحويل الكتلة الحيوية؛ التحسين؛ من هجية سطح الاستجابة؛ تنقية مياه الصرف الصحي

الاستجابة؛ تنقية مياه الصرف الصحي

Introduction

Increased technology has benefited man's life on Earth by making it simpler for him, but it has also brought its own set of issues, particularly in terms of pollution. The emission of coloured wastewater endangers the ecology and has sparked widespread concern. Golden yellow GK is a synthetic anthraquinone vat dye used in the dyeing of cotton, rayon, and wool by textile companies (Benkhaya *et al.*, 2020; Jahan *et al.*, 2017). Vat dyes are carcinogenic and poisonous (Choudhury, 2018; Igwegbe *et al.*, 2016; Igwegbe *et al.*, 2020). When dyes are prevalent in the aquatic environment, they obstruct light transmission and so disrupt biological metabolic processes. As a result, it is critical to cleanse effluents containing these colours before discharging them into the environment.

To remove colours from wastewater, several treatment methods have been used, including coagulation-flocculation, electrocoagulation, adsorption, and advanced oxidation processes. However, the adsorption technique is the most often utilised approach for colour removal (Al-Gheethi *et al.*, 2022; Katheresan *et al.*, 2018). Adsorption may be divided into two types: physisorption (which occurs owing to van der Waals forces and is reversible) and chemisorption (due to covalent or ionic bond) (Huber *et al.*, 2019; Saleh, 2022).

Adsorbents derived from agricultural wastes exceed other adsorbents because they are less expensive and more easily accessible, and they may be utilised without or with minimal processing, lowering the cost of manufacture and the energy required for heat treatment (C. Igwegbe *et al.*, 2021; Onyechi, 2014; Umembamalu *et al.*, 2020). African pear is an African fruit tree, widespread in several Sub-Saharan nations (Kehlenbeck *et al.*, 2013).

By selecting the ideal experimental settings, response surface methodology (RSM) can decrease the number of costly experiments. As a result, response surface methodology (RSM) may be utilised to solve an optimization issue with the objective of maximising the percentage elimination. The experimental design has also been effectively used in many processes for optimisation. Little or no study has reported the optimisation of the removal of this particular dye.

Therefore, the goal of this research is to enhance the adsorption process for removing GY dye from aqueous solutions using CAPS. The studies for GY adsorption on CAPS were designed using a central composite design (CCD). The RSM method was used to study the most effective process parameters, their interactions, and the best conditions for GY elimination. The RSM and artificial neural network (ANN) approaches were used to simulate the process, and their predictive capabilities were compared via the R^2 and functional statistical error values.

Experimental materials and methods

Materials

LOBA Chemie PVT LTD., India, supplied the Golden Yellow GK (purity: 99.99%) (**Fig. 1**). All solutions were made with double-distilled water. The compounds were utilised in their unpurified state.

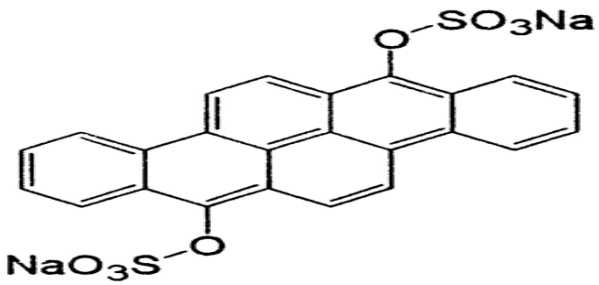

Figure 1. *Molecular structure of GY*

Adsorbent production

The African pear seeds were gathered in the vicinity of Awka, Nigeria. The seed samples were ripped apart, and the inside little seeds were collected before being cleaned with deionized water to remove debris and dried at 105^0 degrees Celsius for 24 hours. 100 g of the dried sample was soaked in 60% NaCl in a weight ratio of 1:1 at room temperature before being carbonised under nitrogen gas flow for 3 hours in a muffle furnace at 300^0C. The carbonised sample was cooled and rinsed in deionized water until it achieved a pH of 7. Finally, the material (CAPS) was crushed and sieved to 0.6 µm particle size before being kept in a sealed jar.

Characterisation of the adsorbent

The surface structure of CAPS (surface area: 739 m^2/g) was determined using scanning electron microscopy (SEM). The functional groups involved in GY adsorption were also determined using an FTIR-8400s.

Batch adsorption studies:

GY stock solution was made by dissolving a sufficient amount of GY in double-distilled water. The effect of process factors such as pH, adsorbent mass, solution temperature, starting GY concentration, and contact duration on GY adsorption on CAPS was examined. Batch adsorption tests were carried out by introducing 100 mL of dye stock solution (10 mg/l) to 250 mL Erlenmeyer flasks treated with a specified quantity of adsorbent. The solution's pH was changed with 0.1 M NaOH or HCl. The ingredients were shaken for the necessary amount of time at 120 rpm with a stirrer. The solution was then centrifuged and filtered after the required treatment time. The residue concentration was evaluated using a UV-visible spectrophotometer (Model UV 752) at maximum absorbance (419 nm). GY was calibrated to determine the relationship between absorbance and concentration. The quantity of GY

adsorbed on CAPS, qe (mg/g), and the percentage of GY removed, R(%), were calculated as follows:

$$R(\%) = 1 - \frac{C_0}{C_0} X\ 100 \quad (1)$$

$$q_{e\ =} \frac{(C_o - C_e)V}{M} \quad (2)$$

Where q_e represents the equilibrium adsorption capacity (mg/g), C_0 represents the initial concentration of GY in the solution (mg/L), C_e represents the final or equilibrium concentration of GY in the solution (mg/L), V represents the volume of the GY solution (L), and W represents the mass of CAPS (g).

Experimental design

The central composite design (CCD) was used to study the effect of contact duration (min), solution temperature (K), starting pH of the solution, and adsorbent dosage (g) on GY elimination %. (the dependent variable). The independent variables were coded at five levels ranging from -1 to +1 (**Table 1**), which included the centre point (0) and two axial points (- and +). (**Table 1**). This study required 30 experiments and used a CCD experimental design with 5-level variables based on RSM (including 8 axial points, 16 factorial points and 6 replicates at the centre points). The RSM was used to determine the best conditions for the percentage of GY adsorbed on CAPS at 100 mg/L GY concentration. The experiment was carried out in accordance with **Table 2** to maximise GY adsorption on CAPS. The experimental data were analysed and interpreted using Stat - Ease, Inc.'s design expert version 11 software, Minneapolis, MN. The interaction effects of the process parameters and the optimal conditions for the adsorption process were established using ANOVA and response surface plots. The ANOVA method was used to investigate the linear, quadratic, and linear interaction effects of the operational parameters on the percentage of GY adsorbed. The second-order polynomial regression model was used to fit the experimental data (Ahmadi et al. 2021).

Table 1. Experimental range and values of the independent factors used to remove GY from ADSEC.

Independent variables	**Code**	**Coded variable levels**				
		-α	-1	0	+1	+α
Contact time (min)	A	45	60	75	90	105
Solution temperature (K)	B	303	308	313	318	323
pH of the solution	C	2	4	6	8	10
CAPS dose (g)	D	0.25	0.50	0.75	1.00	1.25

The model's adequacy was confirmed by comparing the coefficient of determination, R^2, to the adjusted R^2 value. Using the RSM's numerical optimization, the optimum values of the specified variables were found. The

p-values and Fisher's F values were used to determine the statistical significance of the independent variables. The same application was used to create the response surface plots.

Results and Discussion

Characterization results of the adsorbent

Figure 2a shows an SEM picture of CAPS (4000x). The CAPS has a high porosity, which will offer adsorption sites for GY adsorption. **Figure 2b** depicts the FTIR spectra of CAPS. The presence of C-Br stretching of alkyl halides (503.44 cm^{-1}), C-Cl stretching of alkyl halides (639.42 cm^{-1}), = C - H bending of alkenes (865.10 cm^{-1}), C - O stretching of carboxylic acids, esters, and ethers (1009.77 cm^{-1}), C - C stretching of aromatics (1415.80 cm^{-1}), N - O asymmetric stretching of nitro compounds (1833.40 cm^{-1}), – C ≡≡ C – stretching of alkynes (2265.47 cm^{-1}), and alcohols and phenols O – H stretching (3429.55 and 3874.16 cm^{-1}) was observed on the CAPS. Because of the hydrogen bonding, this O - H bond actively engaged in the adsorption of GY (Parida *et al.*, 2006; Ye *et al.*, 2019).

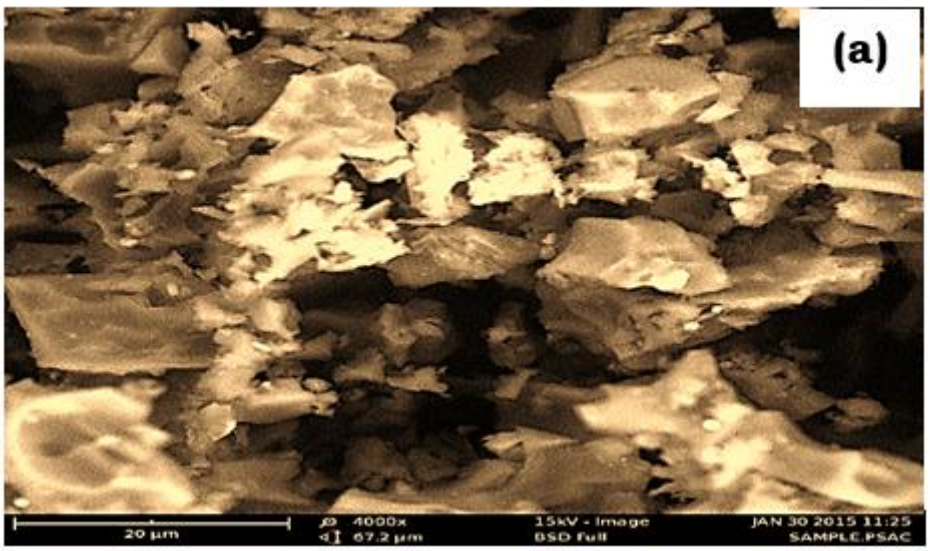

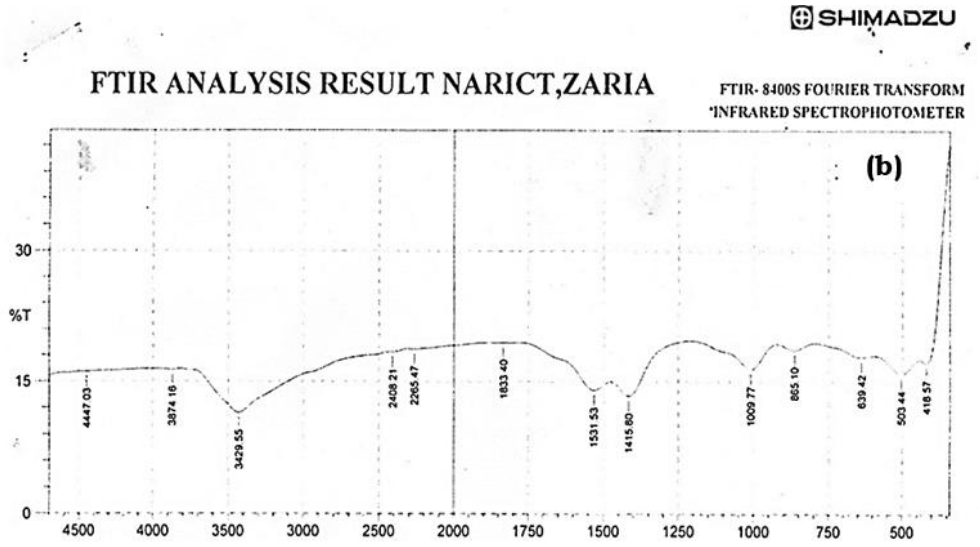

Figure 2. (i) SEM image and (ii) FTIR spectra of the CAPS.

Model fitting and Statistical Analysis of GY adsorption on ADSEC using RSM

Table 2 and **Fig. 3** show the actual and projected GY adsorption percentages. The appropriate correlation, R^2 (0.9879), between the experimental responses of the independent variable and the anticipated values suggested that the model was adequate.

To select the best models, the experimental data were assessed using the sequential model sum of squares and model summary statistics. **Table 3** shows that, with the exception of the cubic model, the quadratic model provided the greatest R^2, adjusted R^2, and anticipated R^2 values when compared to the other models (linear, interactive, and cubic). Because it is aliased, the cubic model cannot be utilised for data modelling (Asaithambi *et al.*, 2018; Maran *et al.*, 2013). An aliased model is caused by inadequate experimental runs to independently evaluate all of the model's parameters.

In addition, the analysis of variance, ANOVA, was employed to assess the relevance of the quadratic regression model and model terms. To analyse the impacts of the operational variables, linear interaction and quadratic effects, the p-value at 95% confidence level and F-value were used as the rulers. A p-value less than 0.05 suggests that a model term has a substantial influence on the process. The ANOVA findings (Table 4) show that the quadratic model derived from the RSM was statistically significant for GY % adsorbed (Y), with an F value of 87.70. F-value this big might arise owing to noise at just 0.01%.

The quadratic model prediction equation for GY adsorption on CAPS (%GP) is shown below:

$$\%\text{GY adsorbed} = 72.92 + 1.39\text{A} + 0.75\text{B} - 7.01\text{C} + 1.80\text{D} - 0.10\text{AB} - 0.014\text{AC} - 0.13\text{AD} - 0.36\text{BC} + 0.30\text{BD}\ 0.056\text{CD} - 2.27A^2 - 1.46B^2 - 3.23C^2 - 0.34D^2 \quad (3)$$

A, B, C, D, A^2, B^2, and C^2 are key model terms in this scenario. Values larger than 0.1000 imply that the model terms are unimportant. If your model has a large number of irrelevant model terms (not including those necessary to enable hierarchy), model reduction may enhance your model. The F-value for "Lack of Fit" of 103.56 indicates that the Lack of Fit is significant. A "Lack of Fit F-value" this significant might arise owing to noise just 0.01% of the time. The F-values of the terms reported in **Table 4** reveal that the pH of the solutions had the greatest influence on the model (F-value = 841.48). Looking at the F-values, the hierarchy of the significance of the factors is pH>CAPS dose>time>temperature. The predicted R^2 of 0.9307 is generally consistent with the Adj. R^2 of 0.9767. Adequate precision larger than 4 is preferred. The ratio of 37.136 suggests that the signal is acceptable. This paradigm is useful for navigating the design space. The low coefficient of variation, CV value of 1.76, indicates that the studies were performed precisely and reliably. Standard deviation of 1.18 was observed between the predicted and the actual observations.

Table 2. Actual and expected values for GY adsorbed (%) on CAPS.

Run	**Contact time (min)**	**Temperature (K)**	**pH**	**Adsorbent dosage (g)**	**GY adsorbed (%)**		
					Actual	*RSM predicted*	*ANN predicted*
1	75	313	6	1.25	75.17	75.84	74.83
2	75	303	6	0.75	65.55	64.93	65.48
3	75	313	6	0.75	73.82	73.41	73.30
4	60	308	4	0.5	65.67	66.42	65.32
5	60	318	4	0.5	69.68	70.08	69.57
6	75	313	6	0.75	74.10	73.41	73.30
7	60	318	8	1	60.99	59.50	60.70
8	90	308	4	0.5	68.68	69.86	68.68
9	60	308	4	1	71.28	71.29	71.39
10	90	308	8	0.5	58.54	57.81	59.43
11	75	313	6	0.75	72.71	73.41	73.30
12	90	318	4	0.5	74.56	74.12	76.38
13	60	318	4	1	74.84	75.14	75.71
14	75	313	10	0.75	43.63	46.34	44.23
15	60	318	8	0.5	56.74	55.66	56.58

16	90	318	4	1	78.33	78.67	78.27
17	75	313	6	0.75	73.91	73.41	73.30
18	45	313	6	0.75	59.56	60.06	59.50
19	75	313	2	0.75	76.01	74.04	75.82
20	75	313	6	0.25	67.56	67.64	67.62
21	75	323	6	0.75	68.24	69.61	68.20
22	75	313	6	0.75	73.00	73.41	73.30
23	90	318	8	0.5	58.96	58.64	58.20
24	60	308	8	1	59.06	59.07	58.71
25	60	308	8	0.5	56.08	55.43	56.04
26	75	313	6	0.75	72.91	73.41	73.30
27	90	318	8	1	63.15	61.97	59.47
28	105	313	6	0.75	65.72	65.96	65.41
29	90	308	4	1	73.57	74.22	73.58
30	90	308	8	1	61.66	60.94	61.85

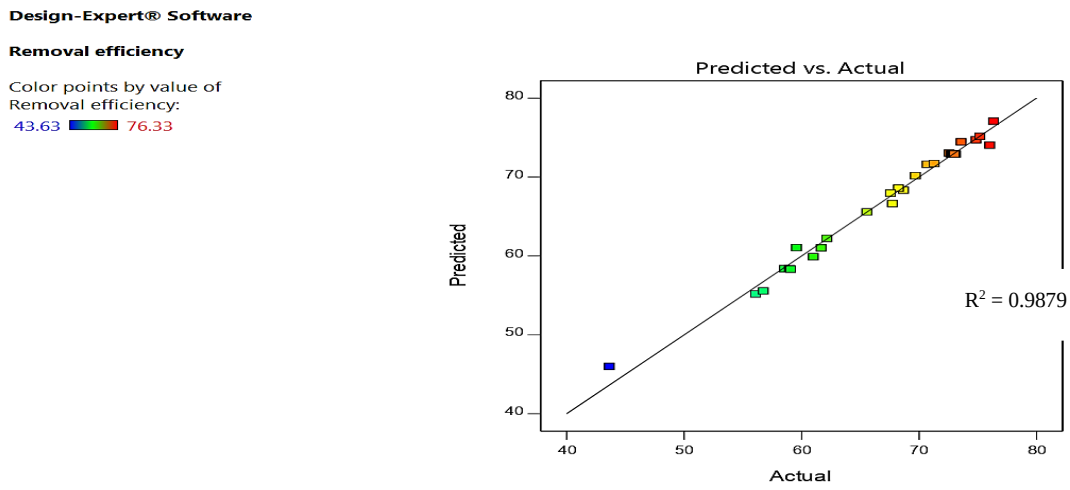

Figure 3. Plot of expected versus actual experimental values for GY adsorption on CAPS.

Table 3. Summary statistics for the model and the sequential model sum of squares for GY adsorption on CAPS.

Sequential model sum of squares						
Source	*Sum of Squares*	*df*	*Mean Square*	*F value*	*P value*	*Prob > F*
Mean vs Total	135000	1	135000			
Linear vs Mean	1316.59	4	329.15	19.4	< 0.0001	
2FI vs Linear	3.93	6	0.66	0.03	0.9999	
Quadratic vs 2FI	399.21	4	99.8	71.25	< 0.0001	Suggested
Cubic vs Quadratic	20.39	8	2.55	28.92	0.0001	Aliased
Residual	0.62	7	0.088			
Total	136800	30	4559.45			
Model summary statistics						
Source	*Std. Dev.*	R^2	*Adjusted* R^2	*Predicted* R^2	*PRESS*	
Linear	4.12	0.7563	0.7173	0.677	562.21	
2FI	4.7	0.7586	0.6315	0.5964	702.61	
Quadratic	1.18	0.9879	0.9767	0.9307	120.58	Suggested
Cubic	0.3	0.9996	0.9985	0.9572	74.46	Aliased

Table 4. ANOVA table for response surface quadratic model.

Source	**Sum of Squares**	**df**	**Mean Square**	**F-value**	**p-value**
Model	1719.73	14	122.84	87.70	< 0.0001
A-Contact time	46.57	1	46.57	33.24	< 0.0001
B-Solution temperature	13.64	1	13.64	9.73	0.0070
C-pH of solution	1178.66	1	1178.66	841.48	< 0.0001
D-CAPS dose	77.72	1	77.72	55.49	< 0.0001
AB	0.1620	1	0.1620	0.1157	0.7385
AC	0.0033	1	0.0033	0.0024	0.9619
AD	0.2576	1	0.2576	0.1839	0.6742
BC	2.04	1	2.04	1.45	0.2464
BD	1.42	1	1.42	1.02	0.3296
CD	0.0495	1	0.0495	0.0353	0.8534
A^2	141.35	1	141.35	100.91	< 0.0001
B^2	58.18	1	58.18	41.53	< 0.0001
C^2	285.29	1	285.29	203.68	< 0.0001
D^2	3.15	1	3.15	2.25	0.1545
Residual	21.01	15	1.40		
Lack of Fit	20.91	10	2.09	103.56	< 0.0001
Pure Error	0.1010	5	0.0202		
Cor Total	1740.74	29			

Std. Dev.: 1.18; C.V. % =1.76; Adeq. Precision = 37.1355; R^2 = 0.9879; Adjusted R^2 = 0.9767; Predicted R^2 = 0.9307

The residual plot in **Fig. 4** reveals a significant degree of correlation. The data points on the plot are in a straight line, thus no data processing is required (Ozturk D. *et al.*, 2017). The box-cox plot is a technique that may be used to

evaluate the best power transformation to apply to response data. Power transformations aid in the enhancement of diagnostic charts and statistical analysis. The box-cox transformation graphic (**Fig. 5**) similarly demonstrates that no data transformation is advised since Lambda = 1.

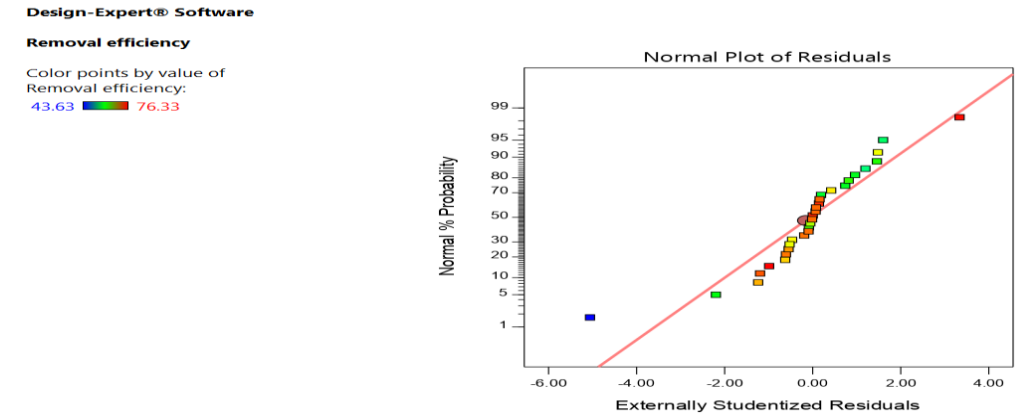

Fig. 4: Plot of normal probability versus residuals for GY adsorbed on CAPS.

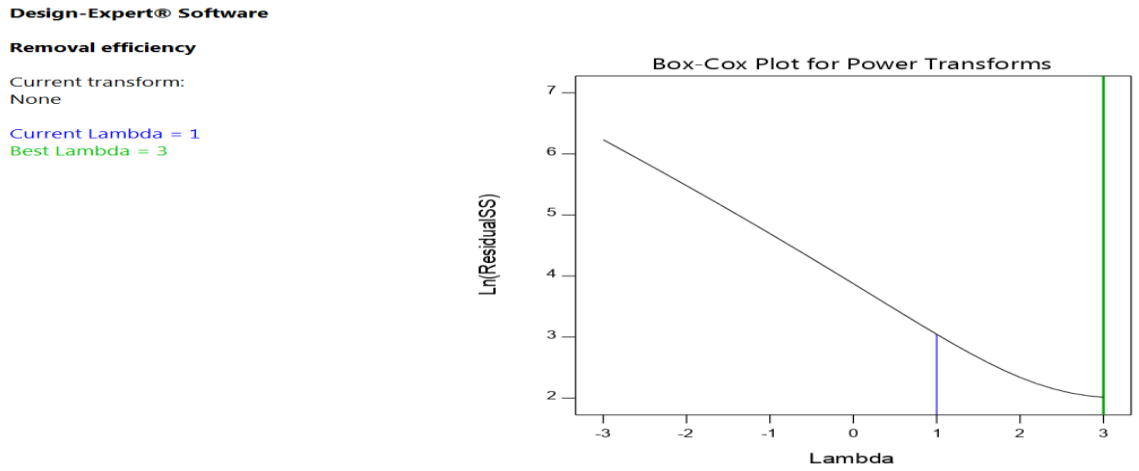

Fig. 5. The box–cox plot for power transforms for GY adsorption onto CAPS.

3.3. Response surface plots

By displaying 3D curves against any two independent process parameters while leaving other variables at their centre (0) level, the individual and interaction impacts of the process factors on the percentage adsorption of GY on CAPS were examined. **Figure 6** demonstrates the 3D curves of the response (% adsorption) between the factors. Positive impacts can be detected in the interactions between the

operational factors at the same time. The pH of a species influences its degree of ionisation, which in turn influences adsorption (Chowdhury *et al.*, 2011). The surface charge of the adsorbent and the state of adsorbate in solution are determined by the pH of the solution (Banerjee and Chattopadhyaya, 2017). As shown in **Figs. 6b, d, f,** the percentage removal increased significantly as the initial pH of the solution increased, indicating that the initial pH of the solution has a very strong influence on GY ac **(a)** on. Higher uptakes at lower p **(b)** may be due to electrostatic attractions between the negatively charged functional groups on the reactive dye surface and the positively charged CAPS surface (Rajput *et al.*, 2017; Vakili *et al.*, 2014). As the adsorbent dose was raised, the percentage adsorbed rose (**Figs. 6c, e, f**). This is because increasing the adsorbent dose increases the number of accessible active sites for adsorption (Umoren *et al.*, 2013). As illustrated in **Figs. 6a, b, c**, the removal increased with increasing contact time. Increased contact duration increases dye mobility during adsorption (Ahmad & Rahman, 2011; Alibak *et al.*, 2022; C. A. Igwegbe, J. O. Ighalo, *et al.*, 2021). **Figures 6a, d, e** demonstrate that raising the system's solution temperature marginally enhanced the adsorption percentage; as a result, higher temperatures aided GY adsorption.

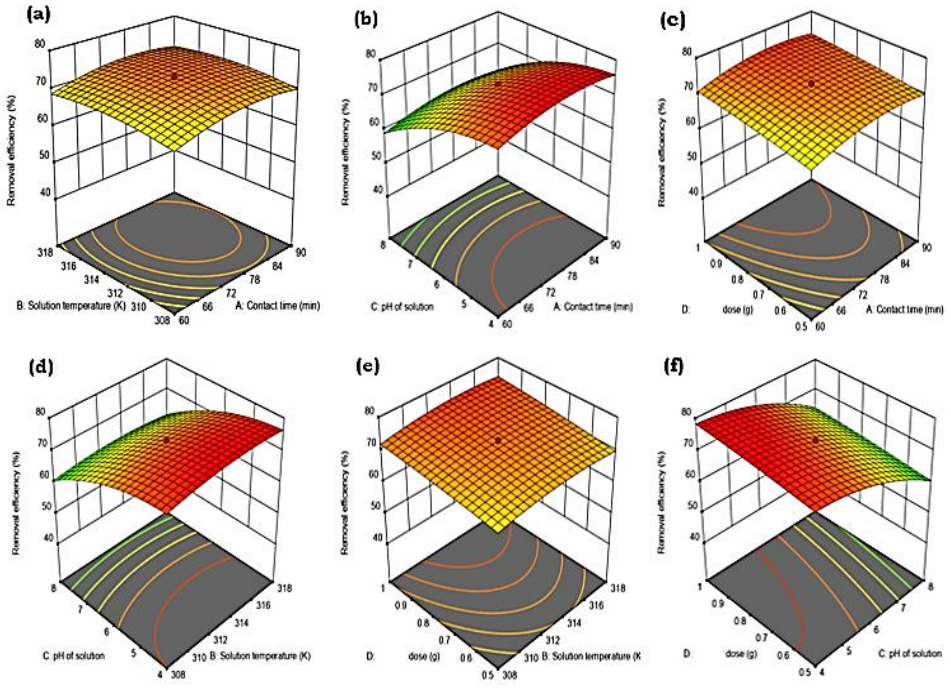

Figure 6: 3D plots of the effect of (a) solution temperature and contact time, (b) initial pH of the solution and contact time, (c) adsorbent dose and contact time,

(d) initial pH of the solution and solution temperature, (e) adsorbent dose and solution temperature, and (f) adsorbent dose and initial pH of solution on CAPS for GY adsorbed (%).

Optimization for GY adsorption

The contact period of 78.13 minutes, solution temperature of 313.57 K, pH of the solution of 4.24, and adsorbent dosage of 0.88 g projected for the 77.77% GY elimination on CAPS resulted in a desirability of 1. This number agrees with the experimental value of 77.93% obtained at the same optimal process variable settings. The attractiveness of a model near to unity (1) and with low error reflects the model's applicability (Shahzad *et al.*, 2017).

Artificial neural network (ANN) modelling

Aside from RSM modelling, data from the ANN **(**artificial intelligence tool) modelling was given. The neural network tool in Matlab 2018a was used for the modelling. As input data, the experimental data set obtained from the experimental design supplied by RSM's CCD was employed. The network was trained using the Multi-Layer Perceptron (MLP) Levenberg-Marquardt (LM) method (MLP). The network was made up of the input layer (which included the five process parameters), neurons (the hidden layer), and the output layer (which contained the removal efficiency %). Based on R^2 and mean square error values, the ideal number of hidden layer neurons was determined by trial and error. The plot of the validation performance (**Fig. 7**), shows how the number of epochs varied with the MSE for the optimal neural network. The best validation performance was 0.39481 at epoch 10. The scatter plots depicting the linearity of the output values of the network with the target values for the training, testing, validation, and overall data (as generated by the MLP platform) were illustrated in **Fig. 8**. The R^2 values were used to indicate the linearity – with the training network having the highest value of 0.99959 for the optimal neural network. The high R^2 value (0.9943) and statistical errors (AAD, RSME and SEP) proved a more adequate correlation than the RSM. The predicted responses at various experimental sets were presented in **Table 2**.

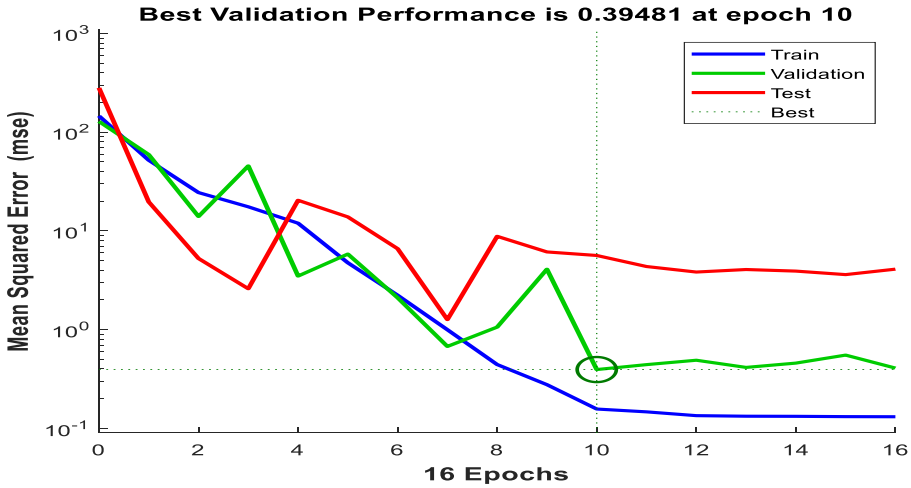

Figure 7. Performance plot for the system.

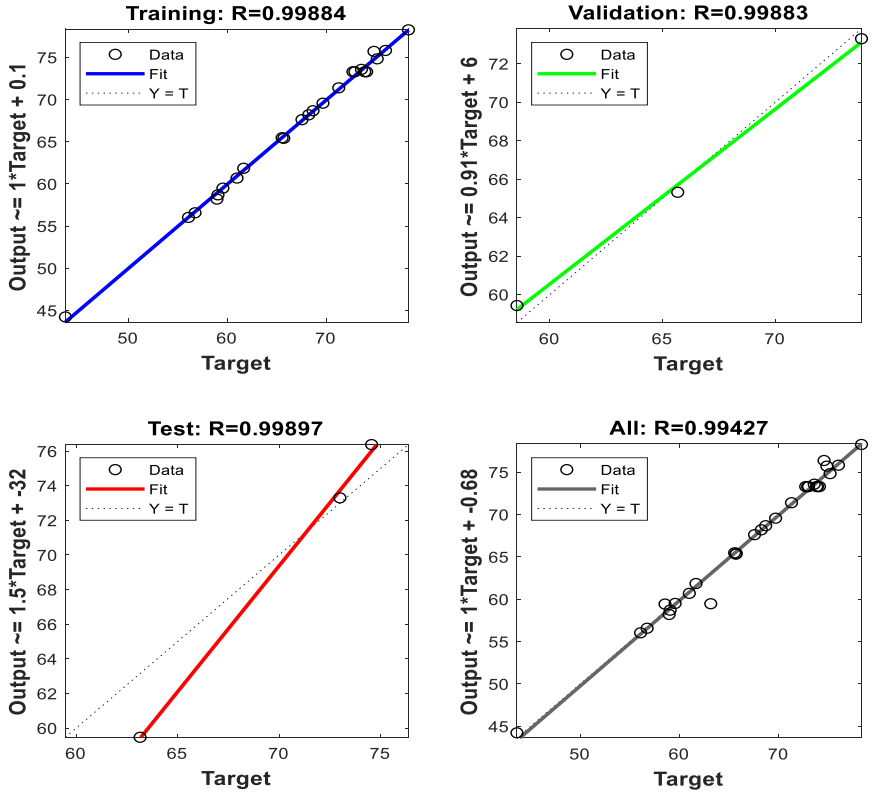

Figure 8.The scatter plots of the output values of the network with the target values for the training, testing, validation, and overall data (as generated by the MLP platform).

Table 5. Error values calculated for RSM and ANN (C. A. Igwegbe, O. D. Onukwuli, et al., 2021).

Statistical error	Equation	RSM	ANN
Absolute average deviation (AAD)	$AAD = [\frac{1}{n}\sum_{i=1}^{n}(\frac{\%R_{i,pred} - \%R_{i,exp}}{\%Ri,_{exp}})]\ X\ 100$	0.0028	0.0015
Root mean squared error (RMSE)	$RMSE = (\frac{1}{n}\sum_{i=1}^{n}(\%R_{i,pred} - \%R_{i,exp})^2)^{1/2}$	0.0146	0.0126
SEP standard error of prediction (SEP)	$SEP = \frac{RMSE}{\lvert\%R_{i,exp}\rvert} \times 100$	0.0220	0.0189

$\%\boldsymbol{R_{i,exp}}$ = Experimental responses; $\%\boldsymbol{R_{i,pred}}$ = Predicted responses

Conclusion

The adsorptive removal of Golden Yellow (GY) on carbon from Activated *Dacroydes edulis* seeds has been investigated. The ideal adsorption process conditions were explored using Central Composite Design based on Response Surface Methodology. Maximum GY removal (77.7669%) was reached under the optimal circumstances of 78.13 min contact time, 313.57K solution temperature, pH 4.24, and 0.88 g adsorbent dosage. The coefficient of determination, R^2 (0.9879), modified R^2 (0.9767), and anticipated R^2 (0.9307) results show that the RSM can characterise the process. The high R^2 value (0.9943) and statistical errors (AAD, RSME and SEP) given by the artificial neural network modelled data depicted adequate correlation than of the RSM. RSM may be used to optimise and characterise the removal of GY from aquatic environments since the experimental (77.93%) at the optimum is close to the predicted (77.77%) value.

Acknowledgment

The authors would like to thank the Nnamdi Azikiwe University Faculty of Engineering in Awka, Nigeria; the National Research Institute for Chemical Technology (NARICT) in Zaria, Nigeria; the National Metallurgical Training Institute in Onitsha, Nigeria; and the Scientific Equipment Development Institute (SEDI) in Enugu, Nigeria.

Disclosure statement

Conflict of Interest: The authors declare that there are no conflicts of interest.

Compliance with Ethical Standards: This article does not contain any studies involving human or animal subjects.

Authors' contributions

Chinenye Adaobi Igwegbe: Conceptualisation, methodology, projection administration, investigation, software analysis, data curation, result analysis, writing -

original draft, writing - review & editing; ***Chinedu Josiah Umembamalu*:** Methodology, software analysis, data curation, writing - original draft, writing - review & editing.

References

Ahmad, M. A., & Rahman, N. K. (2011). Equilibrium, kinetics and thermodynamic of Remazol Brilliant Orange 3R dye adsorption on coffee husk-based activated carbon. *Chemical Engineering Journal*, *170*(1), 154-161. https://doi.org/10.1016/j.cej.2011.03.045

Al-Gheethi, A. A., Azhar, Q. M., Kumar, P. S., Yusuf, A. A., Al-Buriahi, A. K., Mohamed, R. M. S. R., & Al-Shaibani, M. M. (2022). Sustainable approaches for removing Rhodamine B dye using agricultural waste adsorbents: A review. *Chemosphere*, *287*, 132080. https://doi.org/10.1016/j.chemosphere.2021.132080

Alibak, A. H., Khodarahmi, M., Fayyazsanavi, P., Alizadeh, S. M., Hadi, A. J., & Aminzadehsarikhanbeglou, E. (2022). Simulation the adsorption capacity of polyvinyl alcohol/carboxymethyl cellulose based hydrogels towards methylene blue in aqueous solutions using cascade correlation neural network (CCNN) technique. *Journal of Cleaner Production*, *337*, 130509. https://doi.org/10.1016/j.jclepro.2022.130509

Asaithambi, P., Beyene, D., Aziz, A. R. A., & Alemayehu, E. (2018). Removal of pollutants with determination of power consumption from landfill leachate wastewater using an electrocoagulation process: optimization using response surface methodology (RSM). *Applied Water Science*, *8*(2), 1-12. https://doi.org/10.1016/j.jclepro.2022.130509

Banerjee, S., & Chattopadhyaya, M. (2017). Adsorption characteristics for the removal of a toxic dye, tartrazine from aqueous solutions by a low cost agricultural by-product. *Arabian Journal of Chemistry*, *10*, S1629-S1638. https://doi.org/10.1016/j.arabjc.2013.06.005

Benkhaya, S., M'rabet, S., & El Harfi, A. (2020). A review on classifications, recent synthesis and applications of textile dyes. *Inorganic Chemistry Communications*, *115*, 107891. https://doi.org/10.1016/j.inoche.2020.107891

Choudhury, A. K. R. (2018). Eco-friendly dyes and dyeing. *Advanced Materials and Technologies for Environmental*, *2*, 145-176.

Chowdhury, S., Chakraborty, S., & Saha, P. (2011). Biosorption of Basic Green 4 from aqueous solution by Ananas comosus (pineapple) leaf powder. *Colloids and surfaces B: Biointerfaces*, *84*(2), 520-527. https://doi.org/10.1016/j.colsurfb.2011.02.009

Huber, F., Berwanger, J., Polesya, S., Mankovsky, S., Ebert, H., & Giessibl, F. J. (2019). Chemical bond formation showing a transition from physisorption to chemisorption. *Science*, *366*(6462), 235-238. DOI: 10.1126/science.aay34

Igwegbe, C., Umembamalu, C., Osuagwu, E., Oba, S., & Emembolu, L. (2021). Studies on Adsorption Characteristics of Corn Cobs Activated Carbon for the Removal of Oil and Grease from Oil Refinery Desalter Effluent in a Downflow Fixed Bed Adsorption Equipment. *European Journal of Sustainable Development Research*, *5*(1). https://doi.org/10.29333/ejosdr/9285

Igwegbe, C. A., Ighalo, J. O., Onyechi, K. K., & Onukwuli, O. D. (2021). Adsorption of Congo red and malachite green using H_3PO_4 and NaCl-modified activated carbon from rubber (Hevea brasiliensis) seed shells. *Sustainable Water Resources Management*, *7*(4), 1-16. https://doi.org/10.1007/s40899-021-00544-6

Igwegbe, C. A., Onukwuli, O. D., Ighalo, J. O., & Menkiti, M. C. (2021). Bio-coagulation-flocculation (BCF) of municipal solid waste leachate using *Picralima nitida* extract: RSM and ANN modelling. *Current Research in Green and Sustainable Chemistry*, *4*, 100078. https://doi.org/10.1016/j.crgsc.2021.100078

Igwegbe, C. A., Onukwuli, O. D., & Nwabanne, J. T. (2016). Adsorptive Removal of Vat Yellow 4 on Activated Mucuna pruriens (Velvet Bean) Seed Shells Carbon: *Asian Journal of Chemical Sciences* 1(1), 1-16. DOI: 10.9734/AJOCS/2016/30210

Igwegbe, C. A., Onukwuli, O. D., Onyechi, K. K., & Ahmadi, S. (2020). Equilibrium and Kinetics Analysis on Vat Yellow 4 Uptake from Aqueous Environment by Modified Rubber Seed Shells: Nonlinear modelling. *J. Mater. Environ. Sci.*, *11*(9), 1424-1444.

Jahan, R., Arju, S. N., & Nahar, K. (2017). A New Approach to Eco-friendly Dyeing of Cotton Fabric. *BioResources*, *12*, 2496-2506. DOI: 10.30509/PCCC.2022.166915.1141

Katheresan, V., Kansedo, J., & Lau, S. Y. (2018). Efficiency of various

recent wastewater dye removal methods: A review. *Journal of Environmental Chemical Engineering*, *6*(4), 4676-4697. https://doi.org/10.1016/j.jece.2018.06.060

Kehlenbeck, K., Asaah, E., & Jamnadass, R. (2013). Diversity of indigenous fruit trees and their contribution to nutrition and livelihoods in sub-Saharan Africa: examples from Kenya and Cameroon. *Diversifying food and diets: using agricultural biodiversity to improve nutrition and health*, 257-269.

Maran, J. P., Manikandan, S., & Mekala, V. (2013). Modeling and optimization of betalain extraction from Opuntia ficus-indica using Box–Behnken design with desirability function. *Industrial Crops and Products*, *49*, 304-311. https://doi.org/10.1016/j.indcrop.2013.05.012

Onyechi, C. (2014). *Textile wastewater treatment using activated carbon from agro wastes. M. Eng.* Thesis, Department of Chemical Engineering, Nnamdi Azikiwe University, Awka.

Ozturk D., Sahan T., Bayram T., & A., E. (2017). Application of response surface methodology (RSM) to optimize the adsorption conditions of cationic Basic Yellow 2 onto pumice samples as a new adsorbent. *Fresenius Environmental Bulletin*, *26*, 3285-3295.

Parida, S. K., Dash, S., Patel, S., & Mishra, B. (2006). Adsorption of organic molecules on silica surface. *Advances in Colloid and Interface Science*, *121*(1-3), 77-110. https://doi.org/10.1016/j.cis.2006.05.028

Rajput, S., Singh, L. P., Pittman Jr, C. U., & Mohan, D. (2017). Lead (Pb^{2+}) and copper (Cu^{2+}) remediation from water using superparamagnetic maghemite (γ-Fe_2O_3) nanoparticles synthesized by Flame Spray Pyrolysis (FSP). *Journal of Colloid and Interface Science*, *492*, 176-190. https://doi.org/10.1016/j.jcis.2016.11.095

Saleh, T. A. (2022). Adsorption technology and surface science. *Interface Science and Technology* (Vol. 34, pp. 39-64): Elsevier. https://doi.org/10.1016/B978-0-12-849876-7.00006-3

Shahzad, N., Pugliese, D., Cauda, V., Shahzad, M., Shah, Z., Baig, M., & Tresso, E. (2017). Comparative spectroscopic approach for the dye loading optimization of sheet-like ZnO photoanodes for dye-sensitized solar cells. *Journal of Photochemistry and Photobiology A: Chemistry*, *337*, 192-197.

https://doi.org/10.1016/j.jphotochem.2017.01.011

Umembamalu, C. J., Igwegbe, C. A., Osuagwu, E. U., & Nwabanne, J. T. (2020). Packed bed column adsorption of oil and grease from refinery desalter effluent, using rice husks derived carbon as the adsorbent: Influence of process parameters and Bohart–Adams kinetics study. *World News of Natural Sciences, 31*, 155-174.

Umoren, S., Etim, U., & Israel, A. (2013). Adsorption of methylene blue from industrial effluent using poly (vinyl alcohol). *J. Mater. Environ. Sci*, *4*(1), 75-86.

Vakili, M., Rafatullah, M., Salamatinia, B., Abdullah, A. Z., Ibrahim, M. H., Tan, K. B., Gholami, Z., & Amouzgar, P. (2014). Application of chitosan and its derivatives as adsorbents for dye removal from water and wastewater: A review. *Carbohydrate polymers*, *113*, 115-130. https://doi.org/10.1016/j.carbpol.2014.07.007

Ye, S., Yan, M., Tan, X., Liang, J., Zeng, G., Wu, H., Song, B., Zhou, C., Yang, Y., & Wang, H. (2019). Facile assembled biochar-based nanocomposite with improved graphitization for efficient photocatalytic activity driven by visible light. *Applied Catalysis B: Environmental*, *250*, 78-88. https://doi.org/10.1016/j.apcatb.2019.03.004